

Running Head

Role of ETHE1 in amino acid catabolism

Corresponding Author

Tatjana Hildebrandt, Institut für Pflanzengenetik, Leibniz Universität Hannover, Herrenhäuser
Straße 2, 30419 Hannover, Germany, Tel: +49511 762 5290, Fax: +49 511 762 3608, e-mail:
hildebrandt@genetik.uni-hannover.de

Research Area

Biochemistry and Metabolism

Title

The mitochondrial sulfur dioxygenase ETHE1 is required for amino acid catabolism during carbohydrate starvation and embryo development in *Arabidopsis thaliana*

Authors

Lena Krübel, Johannes Junemann, Markus Wirtz, Hannah Birke¹, Jeremy D. Thornton, Luke W. Browning, Gernot Poschet, Rüdiger Hell, Janneke Balk, Hans-Peter Braun, Tatjana M. Hildebrandt²

Institute for Plant Genetics, Leibniz University Hannover, Herrenhäuser Straße 2, 30419 Hannover, Germany (L.K., J.J., H.P.B., T.M.H.); Centre for Organismal Studies Heidelberg, University of Heidelberg, Im Neuenheimer Feld 360, 69120 Heidelberg, Germany (M.W., H.B., R.H.); Metabolomics Core Technology Platform Heidelberg, University of Heidelberg, Im Neuenheimer Feld 360, 69120 Heidelberg, Germany (G.P., R.H.); John Innes Centre, Norwich Research Park, Norwich NR4 7UH, U.K., and The School of Biological Sciences, University of East Anglia, Norwich NR4 7JT (J.D.T., L.W.B, J.B.)

Summary

A mitochondrial pathway oxidizes hydrogen sulfide or persulfides derived from amino acid catabolism to thiosulfate and affects alternative respiration during carbohydrate starvation.

Footnotes

This work was supported by the Deutsche Forschungsgemeinschaft (HI 1471/1-1 to TH).

¹ Present address: CSIRO Plant Industry, Black Mountain Laboratories, Canberra, ACT 2601, Australia

² Corresponding Author; e-mail hildebrandt@genetik.uni-hannover.de

ABSTRACT

The sulfur dioxygenase ETHE1 catalyzes the oxidation of persulfides in the mitochondrial matrix and is essential for early embryo development in *Arabidopsis thaliana*. We investigated the biochemical and physiological function of ETHE1 in plant metabolism using recombinant Arabidopsis ETHE1 and three T-DNA insertion lines with 50-99 % decreased sulfur dioxygenase activity. Our results identified a new mitochondrial pathway catalyzing the detoxification of reduced sulfur species derived from cysteine catabolism by oxidation to thiosulfate. Knockdown of the sulfur dioxygenase impaired embryo development and produced phenotypes of starvation-induced chlorosis during short-day growth condition and extended darkness, indicating that ETHE1 has a key function in situations of high protein turnover such as seed production and the use of amino acids as alternative respiratory substrates during carbohydrate starvation. The amino acid profile of mutant plants was similar to that caused by defects in the electron-transfer flavoprotein/electron-transfer flavoprotein:ubiquinone oxidoreductase complex and associated dehydrogenases. Thus, in addition to sulfur amino acid catabolism ETHE1 also affects the oxidation of branched-chain amino acids and lysine.

INTRODUCTION

Protein recycling is involved in many cellular processes including metabolic regulation and programmed cell death. Damaged or dispensable proteins and entire organelles are degraded to provide carbohydrates and nitrogen for energy production and the synthesis of new material. In plants, this turnover is essential for tissue remodeling during senescence and seed production as well as for survival under nutrient-limiting stress conditions (Li and Vierstra, 2012). Catabolism of the sulfur containing amino acids cysteine and methionine is still largely unknown. Several enzymes have been shown to release sulfur from cysteine. L-cysteine desulfurases (NFS1, NFS2, EC 2.8.1.7) provide persulfide for the biosynthesis of iron-sulfur clusters, thiamine, biotin, and molybdenum cofactor (Van Hoewyk et al., 2008; Balk and Pilon, 2011). β -Cyanoalanine synthase (CAS, EC 4.4.1.9) detoxifies cyanide under consumption of cysteine and releases β -cyanoalanine and sulfide (Hatzfeld et al., 2000). Cytosolic L-cysteine desulfhydrase (DES1, EC 4.4.1.1), and mitochondrial D-cysteine desulfhydrase (D-CDES, EC 4.4.1.15) catalyze beta-elimination reactions of L- or D-cysteine to pyruvate, ammonium, and H₂S (Riemenschneider et al., 2005; Alvarez et al., 2010). Since their expression increases with age, cysteine desulfhydrases have been suggested to be involved in the catabolism of sulfur containing amino acids during senescence (Riemenschneider et al., 2005; Jin et al., 2011).

Recently, several regulatory functions of sulfide in plants have emerged. Sulfide increases drought resistance by inducing stomatal closure (Garcia-Mata and Lamettina 2010; Jin et al., 2011, 2013), and is also protective against other abiotic stresses such as heat and heavy metals (Zhang et al., 2008, 2010; Li et al., 2012). It negatively regulates autophagy and is probably involved in several additional aspects of plant development (Alvarez et al., 2012; Dooley et al., 2013). However, sulfide is also a potent inhibitor of cytochrome c oxidase (COX) and negatively affects plant growth (Birke et al., 2012), making efficient removal of excess sulfide essential for the survival of the plant. Although fixation of sulfide into cysteine contributes substantially to sulfide detoxification, the presence of an additional, so far unknown mechanism in mitochondria was revealed but not further analyzed (Birke et al., 2012).

ETHE1 is a sulfur dioxygenase (SDO, EC 1.13.11.18) that oxidizes persulfides in the mitochondrial matrix and therefore constitutes a good candidate to be involved in plant sulfur catabolism. In *Arabidopsis thaliana* ETHE1 (AT1G53580) is critical for seed production. A loss-of-function mutation causes alterations in the mitochondrial ultrastructure and an arrest of embryo development at early heart stage (Holdorf et al., 2012). However, the precise biochemical and physiological role of ETHE1 in plant mitochondria has not been established.

Mutations in the human homolog *ETHE1* lead to the fatal metabolic disease ethylmalonic encephalopathy (Tiranti et al., 2004). Primary cause for the disease is a disruption of the mitochondrial sulfide detoxification pathway that oxidizes sulfide to either thiosulfate or sulfate in four steps catalyzed by sulfide:quinone oxidoreductase, *ETHE1*, a sulfurtransferase, and sulfite oxidase (Hildebrandt and Grieshaber, 2008; Tiranti et al., 2009). Increased sulfide concentrations in the bloodstream severely damage the vascular endothelium and thus cause the main symptoms of ethylmalonic encephalopathy: rapidly progressive necrosis in the brain, chronic diarrhea, and microangiopathy (Giordano et al., 2012). In addition, sulfide interferes with mitochondrial energy metabolism. It reversibly inhibits COX at low micromolar concentrations (Tiranti et al., 2009) and chronic exposure destabilizes specific COX subunits (Di Meo et al., 2012). *ETHE1* deficiency also affects mitochondrial catabolism of fatty acids and branched-chain amino acids (BCAA), leading to an accumulation of ethylmalonic acid as well as C4 and C5 acylcarnitines and acylglycines (Tiranti et al., 2009; Hildebrandt et al., 2013).

Here we show that in *Arabidopsis* the mitochondrial sulfur dioxygenase *ETHE1* is part of a sulfur catabolic pathway that catalyzes the oxidation of sulfide or persulfides derived from amino acids to thiosulfate and sulfate. *ETHE1* has a key function in situations of high protein turnover such as seed production or unfavourable environmental conditions leading to carbohydrate starvation and the use of amino acids as alternative respiratory substrates.

RESULTS

We analyzed three T-DNA insertion lines of the *AT1G53580* gene to investigate the physiological function of *ETHE1* in *Arabidopsis*. In the mutant line *ethe1-1* the T-DNA is inserted into the 5'UTR 64 bp upstream of the start codon (Fig. 1A) leading to a decrease in *ETHE1* transcript level by 75 % (Fig. 1B). Immuno-labelling showed that only trace amounts of *ETHE1* protein were present in purified mitochondria of this line (Fig. 1C). In *ethe1-2* and *ethe1-3* the T-DNA insertion is localized in the promoter region of the gene (335 and 327 bp upstream of the start codon, Fig. 1A). *ETHE1* transcript level was 60 to 70 % of the wild type and *ETHE1* protein abundance was also decreased in these lines (Fig. 1B-C).

Sulfur dioxygenase (SDO) activity was measured as oxygen consumption upon addition of 1 mM reduced glutathione (GSH) and elemental sulfur (S_8) using a Clarke-type oxygen electrode. The S_8 sulfur rings react with GSH non-enzymatically to form polysulfane compounds (GSS_nH) including glutathione persulfide (GSSH), the substrate of the SDO

reaction (Rohwerder and Sand, 2003). Mitochondria isolated from wild type Arabidopsis cell suspension culture had an SDO activity of $36.0 \pm 8.4 \text{ nmol O}_2 \text{ min}^{-1} \text{ mg protein}^{-1}$ under standard conditions, which was comparable to the SDO activity in mitochondria isolated from wild type rosette leaves ($44.2 \pm 2.7 \text{ nmol O}_2 \text{ min}^{-1} \text{ mg protein}^{-1}$, $n = 3$). By contrast, almost no SDO activity was detectable in mitochondria from the *ethe1-1* line, and the activity was decreased by 24 % and 64 % in *ethe1-2* and *ethe1-3*, respectively (Fig. 1 D).

The *ETHE1* gene excluding the mitochondrial targeting sequence was expressed in *E. coli* and purified using a C-terminal 6xHis tag. Recombinant Arabidopsis ETHE1 protein had a specific activity of $35.3 \pm 1.8 \text{ } \mu\text{mol O}_2 \text{ min}^{-1} \text{ mg protein}^{-1}$ in the standard activity test for SDO which is 1000 times higher than in isolated mitochondria. The pH optimum of Arabidopsis ETHE1 was around pH 9.0 and the temperature optimum at 55 °C compared to pH 7.5 and 35 °C for human ETHE1 (Supp. Fig. 1 B,C). These results confirm that ETHE1 in Arabidopsis is a sulfur dioxygenase (EC 1.13.11.18).

ETHE1 oxidizes glutathione persulfide to sulfite

Recombinant Arabidopsis ETHE1 was highly specific for GSSH as a substrate. SDO activity comparable to the standard assay using GSH and S₈ as a substrate was only observed in the presence of oxidized glutathione (GSSG) and sulfide, which also form GSSH in a non-enzymatic reaction (Fig. 2A). Free sulfide or 3-mercaptopyruvate were not oxidized, and GSH could not be replaced by other thiols such as cysteine, 3-mercaptoethanol, or dithiothreitol (Supp. Tab. S1).

Human ETHE1 is known to catalyze the reaction $\text{GSSH} + \text{O}_2 + \text{H}_2\text{O} \rightarrow \text{GSH} + \text{SO}_3^{2-} + 2 \text{H}^+$ (Kabil and Banerjee, 2012). To confirm that sulfite (SO₃²⁻) is also the product of ETHE1 in Arabidopsis, we measured thiol levels during the course of the SDO activity assay (Fig. 2B). Sulfite was only detected after addition of S₈, and increased proportionately to the oxygen consumed. The total amount of sulfite produced, which was limited by 250 nmol of oxygen available in the electrode chamber, was $218 \pm 42.4 \text{ nmol}$ ($n = 4$). Thiosulfate was not produced by recombinant ETHE1.

ETHE1 is part of a mitochondrial sulfur catabolic pathway

To test which sulfur compounds can serve as substrates for the ETHE1 dependent pathway we measured oxygen consumption by isolated mitochondria upon addition of a range of potential substrates (Fig. 2C, Supp. Tab. S1). In order to discriminate between ETHE1 dependent oxygen consumption and other mitochondrial reactions we compared activities in wild type

samples to *ethe1-1* and *ethe1-3*. In agreement with the identified substrates for recombinant ETHE1, specific SDO activity could be observed in isolated mitochondria after the addition of GSH and S₈ or GSSG and sulfide (Fig. 2C). Interestingly, the presence of 3-mercaptopyruvate also resulted in a significant rate of oxygen consumption in wild type mitochondria, which was absent in *ethe1-1* and strongly decreased in *ethe1-3* mitochondria, indicating that this reaction is ETHE1 dependent (Fig. 2C). Sulfide or thiosulfate was not oxidized by the mitochondria, whereas L- or D-cysteine addition led to a low rate of ETHE1 independent oxygen consumption (Supp. Tab. 1).

The main product of mitochondrial GSSH oxidation was thiosulfate (Fig. 2D). During the standard activity test using GSH and S₈ as a substrate (0.25 mg/ml mitochondrial protein, 15 min) mitochondria produced $55 \pm 18 \mu\text{M}$ thiosulfate and $9 \pm 10 \mu\text{M}$ sulfite while consuming $103 \pm 25 \mu\text{M}$ oxygen (n = 5). Thus, most of the sulfite produced by the SDO reaction is immediately converted to thiosulfate in Arabidopsis mitochondria, similar to the pathway in animals (Hildebrandt and Grieshaber, 2008).

The mitochondrial sulfur catabolic pathway is involved in sulfide detoxification

To test a potential role of ETHE1 in the detoxification of excess hydrogen sulfide *in vivo*, wild type and *ethe1-1* plants were exposed to a sub-lethal concentration of H₂S (1 ppm) for 12 days. We measured leaf contents of cysteine and GSH, which are produced from sulfide during the sulfur assimilation pathway, as well as of the cysteine precursor *O*-acetylserine (OAS). In addition, the inorganic products of sulfide oxidation thiosulfate, sulfite, and sulfate were analyzed (Fig. 3). Under control conditions *ethe1-1* plants had significantly higher contents of cysteine, GSH and sulfate than the wild type, but decreased levels of thiosulfate and OAS.

In wild type plants, H₂S exposure resulted in a 5-fold increase of the endogenous sulfide concentration. Cysteine and GSH accumulated with a concomitant decrease in the precursor OAS indicating that part of the excess sulfide was incorporated into amino acids. In addition, we found evidence for sulfide oxidation. Concentrations of thiosulfate, sulfite and sulfate were significantly higher in H₂S treated than in control plants. Thiosulfate increased most drastically (1588fold) from 3.8 ± 0.3 to $6002 \pm 117 \text{ pmol mg}^{-1} \text{ FW}$ so that after the H₂S exposure it became one of the most abundant sulfur compounds present in the leaves. The accumulation of thiosulfate and sulfite upon sulfide exposure was significantly less pronounced in *ethe1-1* plants than in the wild-type, and the sulfate concentration even decreased, indicating a role of the ETHE1 dependent mitochondrial sulfur catabolic pathway

in sulfide oxidation. Thus, the results of *in planta* analysis of *ethe1* mutants are in full agreement with the biochemical characterization of ETHE1 recombinant protein and isolated mitochondria and demonstrate the relevance of ETHE1 for detoxification of sulfide derived from cysteine degradation.

Low levels of ETHE1 are sufficient for survival of Arabidopsis plants but development is delayed

While complete knockout of the *ETHE1* gene is embryo lethal (Hohldorf et al., 2012), seeds of the strong knockdown mutant *ethe1-1* were viable. However, we observed a severe delay in embryo development (Fig. 4 A,B). Five days after pollination most of the *ethe1-1* embryos were still at globular stage and reached heart stage only seven days after pollination, whereas wild type embryos were already at heart stage and bent cotyledon or mature stage, respectively. Development of *ethe1-1* plants grown under long-day conditions was also delayed (Fig. 4 C-D). Growth rates of *ethe1-1* rosettes expressed as diameter and number of leaves were about 60 % of the wild type (Supp. Fig. S2). There were no apparent differences regarding embryo development or growth phenotype between wild type plants and the weaker knockdown lines *ethe1-2* and *ethe1-3*.

ETHE1 is involved in mitochondrial amino acid catabolism

We used the information available from a proteomic approach in combination with co-expression analysis to elucidate, in which physiological context ETHE1 activity is most relevant for plant metabolism. Mitochondria isolated from wild type and *ethe1-1* cell suspension cultures were analyzed by IEF/SDS-PAGE, and 73 proteins were identified in 45 spots with a significantly changed volume (Tab. 1, Supp. Fig. S3, Supp. Tab. S2).

Our results confirm the predicted role of ETHE1 in plant sulfur metabolism. Several enzymes involved in cysteine synthesis (serine acetyltransferase, serine hydroxymethyltransferase) or degradation (beta-cyanoalanine synthase, aspartate aminotransferase, NSF1, NFU4, NFU5) were affected in *ethe1-1* mitochondria. Interestingly, we also found indications for differences in energy metabolism between *ethe1-1* and the wild type. TCA cycle dehydrogenases (malate dehydrogenase, succinate dehydrogenase, subunits of pyruvate and 2-oxoglutarate dehydrogenase complexes) as well as enzymes involved in the oxidation of amino acids as alternative substrates of the mitochondrial respiratory chain (e.g. electron-transfer flavoprotein (ETF), ETF: ubiquinone oxidoreductase (ETFQO), branched-chain alpha keto acid dehydrogenase, fumarylacetoacetate hydrolase, methylcrotonoyl-CoA carboxylase,

glutamate dehydrogenase) were detected in spots with a changed volume (Tab. 1). This dataset provides valuable information about which mitochondrial pathways in general are affected by the *ETHE1* knockdown. However, care must be taken not to over-interpret the results. Regulation patterns of individual enzymes cannot be concluded since spot volume is not always equivalent to the total abundance of one specific protein.

The potential role of *ETHE1* in amino acid catabolism is further supported by co-expression analysis using Genevestigator (www.genevestigator.com). *ETHE1* expression was up-regulated in experiments that stimulate nutrient remobilization such as prolonged darkness, drought, abscisic acid treatment, and germination. Enzymes involved in protein degradation and amino acid catabolism as well as peroxisomal fatty acid β -oxidation were most clearly co-expressed with *ETHE1* under these conditions (Supp. Tab. S3). In particular, several enzymes of the BCAA and lysine catabolic pathway (ETF, isovaleryl-CoA dehydrogenase, 3-hydroxyisobutyrate dehydrogenase, branched-chain alpha-keto acid dehydrogenase subunits, aminoadipate-semialdehyde dehydrogenase) showed an expression pattern similar to *ETHE1*. Thus, equivalent to the situation in animals, Arabidopsis *ETHE1* is probably involved in sulfur metabolism as well as mitochondrial amino acid oxidation.

***ETHE1* has an essential function in the use of amino acids as respiratory substrates during carbohydrate starvation**

Identification of a potential role of *ETHE1* in amino acid catabolism prompted us to further investigate the phenotype and amino acid profiles of *ethe1-1* compared to wild type plants under conditions with increased protein degradation. These include senescence, decreased light availability (short-day conditions), and severe carbohydrate starvation caused by extended darkness (Fig. 5). The *ethe1-1* mutant was sensitive to changes in the photosynthetically active period, showing premature senescence under light-limiting conditions. When the plants were grown under long-day conditions (16h light/8h dark), rosette leaves of *ethe1-1* plants appeared pale green compared to the wild type, but otherwise senescence proceeded in a similar fashion (Fig. 5A, Supp. Fig. S4A). Under short-day conditions (8h light/ 16h dark), the oldest leaves of *ethe1-1* plants became chlorotic after seven weeks of growth starting at the edges (indicated by arrows in Fig. 5B). In the further course of development, leaves of the mutant plants turned upwards and showed progressive signs of senescence, while wild type rosettes continued to grow and stayed dark green (Supp. Fig. S4B). This phenotype became more pronounced when plants were grown in extended darkness (Fig. 5C).

To test whether an increase in ROS production contributes to premature leaf senescence in *ethe1-1* plants, we analyzed hydrogen peroxide and superoxide levels in young leaves of plants grown under short-day conditions by DAB and NBT-staining, respectively (Supp. Fig. S5). H₂O₂ production was not significantly different in *ethe1-1* compared to the wild type and clearly restricted to necrotic leaf areas (Supp. Fig. S5A). In contrast, NBT-stained portions of *ethe1-1* leaves (37 ± 26 %) were significantly larger than in the wild type (19 ± 9 %) and not correlated to visible signs of senescence. Interestingly, formazan production is not specific for superoxide, but NBT is also rapidly reduced by GSSH (Supp. Fig. S5D). Thus, our results indicate a general increase in reactive oxygen or sulfur species in *ethe1-1* plants.

In agreement with the postulated function of *ETHE1* in protein catabolism, we found an accumulation of all detectable amino acids in seeds from *ethe1-1* plants compared to the wild type during early embryo development (4-5 DAP) resulting in a 1.8-fold increase of total free amino acid content (Supp. Tab. S4). The amino acid composition was not changed in senescent rosette leaves of *ethe1-1* plants grown under long-day conditions (Fig. 5D, Supp. Tab. S5). However, under short-day conditions concentrations of the compounds related to sulfur metabolism (cysteine, glutathione and serine) as well as the BCAA valine, leucine and isoleucine were significantly higher in the mutant than in the wild type (Fig. 5D, Supp. Tab. S5). The effect on amino acid content became more pronounced when plants were subjected to complete darkness for seven days. The largest differences between *ethe1-1* and the wild type again occurred in sulfur containing amino acids (2- to 5-fold) and BCAA (3- to 6-fold). In addition, extended darkness generally led to a drastic (50- to 60-fold) increase in the nitrogen-rich amino acids arginine and asparagine, and concentrations were slightly higher in *ethe1-1* than wild type leaves (Supp. Tab. S5). As a consequence, the total concentration of free amino acids increased 4-fold in wild type and 5-fold in *ethe1-1* leaves compared to short-day conditions, resulting in a significantly higher total amino acid concentration in mutant than in wild type plants (65.3 ± 7.9 vs. 47.6 ± 8.8 nmol mg FW⁻¹). Surprisingly, there were no significant differences in the contents of sulfide, thiosulfate, or sulfite between wild type and mutant plants upon extended dark treatment (Supp. Tab. S6).

To better characterize the effect of *ETHE1* knockdown on energy metabolism, we analyzed leaf carbohydrate and adenylate levels (Fig. 5D, Supp. Tab. S5). As expected, starch was almost completely depleted after seven days of darkness in wild type and mutant plants, and concentrations of sucrose as well as several monosaccharides also significantly decreased. Differences in metabolite contents between *ethe1-1* and the wild type were again most pronounced in the dark-treated plants. Levels of starch, sucrose, glucose and fructose as well

as total adenylate concentrations (ATP, ADP, AMP) were elevated in *ethe1-1* compared to wild type leaves. However, the AMP/ATP ratio, an indicator of low cellular energy status, was also significantly higher in *ethe1-1* than in wild-type plants under short-day conditions and extended darkness (Fig. 5D).

Together with the strong phenotypic effects, the changes in the metabolite profile of mutant plants point towards a pivotal role of ETHE1 during dark induced carbohydrate starvation. In agreement with this, transcript amount of *ETHE1* was 6.5-fold higher in rosette leaves of wild type plants subjected to extended darkness compared to leaves of plants grown under long- or short-day conditions (Fig. 5E).

DISCUSSION

Plant ETHE1 has recently been identified as a sulfur dioxygenase localized in the mitochondria with an essential but as yet undefined function in early embryo development (Hohldorf et al., 2012). Here we describe the physiological role of ETHE1 in the catabolism of sulfur containing and branched-chain amino acids based on the analysis of three Arabidopsis knockdown mutants. T-DNA insertion into the 5'UTR in *ethe1-1* resulted in a strong decrease in enzyme activity to about 1 % of wild type levels, which was sufficient for plant viability but led to pronounced growth defects throughout the life cycle. A decrease in SDO activity by about 50 % in *ethe1-2* and *ethe1-3* was tolerated by the plants without any obvious phenotypic effects.

The biochemical function of ETHE1: Sulfur oxidation during cysteine catabolism

Increased concentrations of cysteine, methionine and GSH in *ethe1* knockdown plants indicate a function of ETHE1 in sulfur amino acid metabolism. We performed biochemical studies on plants, isolated mitochondria, and recombinant ETHE1 enzyme to investigate details of this function. Our results identified a new mitochondrial pathway catalyzing the detoxification of sulfide or reduced sulfur species derived from cysteine catabolism by oxidation to thiosulfate (Fig. 6).

In plants, free sulfide is normally rapidly incorporated into cysteine by the different OAS-TL isoforms (Hell and Wirtz, 2011). However, an alternative route is required for the degradation of sulfur containing amino acids. Exposure of Arabidopsis plants to environmental H₂S demonstrated that thiosulfate is a major product of sulfide detoxification and ETHE1 is involved in its production. Since thiosulfate was also the main product of persulfide oxidation

in Arabidopsis mitochondria, we postulate that, analogous to the reaction sequence in animals, a sulfurtransferase converts the sulfite produced by *ETHE1* to thiosulfate. According to our results, cysteine catabolism in plants most likely involves transamination to 3-mercaptopyruvate, which is then oxidized by the *ETHE1* pathway. The thiol group is probably transferred from 3-mercaptopyruvate to GSH since *ETHE1* is highly specific for GSSH as a substrate, and this reaction could be catalyzed by mercaptopyruvate sulfurtransferase. A functional connection between *ETHE1* and the main mitochondrial sulfurtransferase *STR1* (AT1G79230) in Arabidopsis is supported by the phenotype of knockout mutants. *STR1* deficiency leads to a delay in early embryo development similar to *ETHE1* deficiency (Mao et al., 2011).

Alternatively, cysteine degradation could proceed via desulfhydration to sulfide, pyruvate and ammonia by the cytosolic L-cysteine desulfhydrase *DES1* (AT5G28030), which has been shown to regulate cysteine homeostasis during senescence and environmental stress (Alvarez et al., 2010). However, we found that Arabidopsis mitochondria were not able to oxidize sulfide, and there is no homolog of the enzyme catalyzing sulfide oxidation in animals, sulfide:quinone oxidoreductase, encoded by plant genomes. Thus, in Arabidopsis the first oxidation step of sulfide to persulfide is either catalyzed by a currently unknown cytosolic enzyme or depends on non-enzymatic GSSH production in the presence of GSSG.

The physiological context of *ETHE1*: amino acid catabolism for ATP production

Several lines of evidence indicate that in addition to its role in cysteine catabolism *ETHE1* is probably involved in energy metabolism and the use of amino acids as alternative respiratory substrates during carbohydrate starvation. Under conditions of low sugar availability such as extended darkness, drought or extreme temperatures, fatty acids are oxidized by peroxisomal β -oxidation and in addition cellular proteins and entire organelles are degraded by autophagy to produce amino acids as an energy source (Araujo et al., 2011). Especially BCAA, aromatic amino acids, and lysine have a key function as substrates for ATP production (Izumi et al., 2013). The pathways oxidizing these amino acids are localized in the mitochondria and transfer electrons into the respiratory chain via the electron-transfer flavoprotein (ETF)/ETF: ubiquinone oxidoreductase (ETFQO) complex (Taylor et al., 2004; Araujo et al., 2010).

Co-expression analysis as well as mitochondrial proteomics clearly placed *ETHE1* in the functional context of carbohydrate starvation, and *ETHE1* expression was indeed induced by extended darkness. In agreement with these results, phenotypic defects of *ETHE1* knockdown plants were more pronounced under light limiting conditions. Plants developed starvation-

induced chlorosis, which is similar to the phenotype produced by defects in autophagy or the ETF/ETFQO system and associated dehydrogenases (Ishizaki et al., 2005, 2006; Araujo et al., 2010; Izumi et al., 2013). The amino acid profile of *ethe1* mutants, which in addition to an accumulation of sulfur amino acids revealed an increase in BCAA characteristic for alternative respiration defects, suggests a specific role of ETHE1 in this pathway. Although premature chlorosis and leaf senescence clearly indicate energy shortage, depletion of starch, sugar and ATP was not accelerated in *ethe1-1* plants. Similar findings from previous studies demonstrate that metabolic adaptations to energy deprivation in plants can be complex. Low concentrations of malate and fumarate lead to accelerated dark induced senescence in a malic enzyme overexpressing Arabidopsis line, while sugar levels are high (Fahnenstich et al., 2007). Down-regulation of different respiratory chain complexes restricts growth despite unchanged or even increased steady-state ATP levels (Szal et al., 2008; Robinson et al., 2009; Geisler et al., 2012). The high AMP/ATP ratio in *ethe1-1* plants could induce a broad transcriptional response to stress and energy deprivation mediated by AMP-activated protein kinases such as KIN10 (AT3G01090), which is co-expressed with *ETHE1* (Baena-Gonzalez et al., 2007).

The amino acid profile of young *ethe1-1* seeds is again strikingly similar to defects in isovaleryl-CoA dehydrogenase, which is involved in the degradation of BCAA (Gu et al., 2010). In contrast to knockout mutants for lysine-ketoglutarate reductase/saccharopine dehydrogenase or threonine aldolase, which very specifically accumulate lysine or threonine in the seeds (Zhu et al., 2001; Jander et al., 2004), isovaleryl-CoA dehydrogenase deficiency leads to a general increase in free amino acids similar to ETHE1 deficiency (Gu et al., 2010). Thus, BCAA catabolism plays an important role in regulating amino acid levels in seeds, and inhibition of this pathway in *ethe1* mutants might interfere with the nutrient supply to the developing embryo. However, since defects in embryogenesis are not described for any of the mutants related to autophagy or the use of amino acids as respiratory substrates (Ishizaki et al., 2005, 2006; Araujo et al., 2010; Gu et al., 2010; Izumi et al., 2013), the severe consequences of ETHE1 deficiency indicate additional problems. Lack of the mitochondrial sulfurtransferase STR1, which we suggest is involved in the same pathway as ETHE1, also impairs embryogenesis (Mao et al., 2011). Thus, seed abortion seems to be an immediate consequence of the block in sulfur catabolism possibly caused by an increase in toxic intermediates such as sulfide or reactive persulfide compounds. This hypothesis will have to be tested e.g. with *ethe1/str1* double mutants. In humans suffering from ethylmalonic encephalopathy C4 and C5 acylcarnitines and acylglycines accumulate in the bloodstream,

indicating a block in fatty acid and branched-chain amino acid oxidation at the level of acyl-CoA. Indeed, H₂S has been shown to inhibit short-chain acyl-CoA dehydrogenase *in vitro* so that the increase in tissue sulfide concentrations caused by ETHE1 deficiency is thought to be responsible for the metabolite profile of the patients (Tiranti et al., 2009). However, sulfide concentrations were normal in *ethe1-1* leaves. Another possible explanation is the inhibition of acyl-CoA dehydrogenases by CoA persulfides (Shaw and Engel, 1987), which are likely to accumulate when high concentrations of reduced sulfur are present. The increased intensity of NBT-staining in *ethe1-1* leaves without changes in hydrogen peroxide production indicate that the block in persulfide oxidation probably leads to an accumulation of reactive sulfur species. Indirect pleiotropic effects such as a decrease in respiratory chain activity and inactivation of additional enzymes by increased ROS levels could also play a role. Proteome studies on ETHE1 deficient mice have further indicated a possible regulatory effect via post-translational protein modifications (Hildebrandt et al., 2013). Thus, our results clearly demonstrate the central function of Arabidopsis ETHE1 in metabolic adaptation to prolonged darkness. Additional experiments will be necessary to clarify mechanistic aspects and distinguish between a direct role of ETHE1 in BCAA catabolism versus general effects on energy homeostasis.

CONCLUSIONS

In summary, the present study identified the physiological role of ETHE1, which is in amino acid catabolism. The sulfur dioxygenase detoxifies reactive intermediates in the degradation of sulfur containing amino acids and strongly affects the oxidation of branched-chain amino acids as alternative respiratory substrates in situations of carbohydrate starvation. Therefore, ETHE1 is expected to be relevant for plant productivity during seed production as well as for stress tolerance against e.g. drought or shading.

MATERIALS AND METHODS

Plant material and growth conditions

All *Arabidopsis thaliana* plants used for this study were of the Columbia ecotype (Col-O). Plants were grown in climate chambers under long-day conditions (16h light/8h dark) or short-day conditions (8h light/16h dark) at 22 °C, 85 μmol s⁻¹ m⁻² light and 65 % humidity. The T-DNA insertion lines SALK_021573 (*ethe1-1*), SALK_091956 (*ethe1-2*), and SALK_127065 (*ethe1-3*) for the gene AT1G53580 were obtained from the Nottingham Arabidopsis Stock Centre (University of Nottingham, UK).

Plants for fumigation experiments were germinated and grown on soil under short day conditions. 3-week-old plants were transferred into fumigation cabinets to allow acclimatization for one week. Subsequently plants were exposed to sulfide (1 ppm H₂S) for 12 days according to Buchner et al. (2004).

For dark treatment, plants were grown under short-day conditions for 7 weeks and then transferred to darkness for 7 days. Before and after the dark treatment, complete rosettes of 5 wild type and mutant plants were harvested and used for metabolite analysis.

Isolation of T-DNA insertion mutants and genotype characterization

Homozygous mutant lines were identified by genomic PCR using gene-specific primers (5'-TGGAATTGGGTTATATGGTGG-3' and 5'-CGGATCAATCAACTGCTCATC-3' for *ethe1-1*, 5'-TGGAATTGGGTTATATGGTGG-3' and 5'-CCCATGTGCGAAAAATTCAATC-3' for *ethe1-2*, 5'-TCATGGATTTCGTGGTATAACCG-3' and 5'-CGGATCAATCAACTGCTCATC-3' for *ethe1-3*) and the T-DNA left border primer LBb1.3 (5'-ATTTTGCCGATTTCGGAAC-3'). PCR products were sequenced by SeqLab (Göttingen, Germany) to determine the exact T-DNA insertion sites. ETHE1 expression was analyzed by quantitative RT-PCR as described in Niessen et al. (2012). Primer combinations were 5'-AAGGTTTCGAGGTAAGTACAGTTGG-3' and 5'-CTTGAGAAGGCACATCTTGTAACC-3' for ETHE1 and 5'-GGAATCTGAAGGCAAAATGAAGG-3' and 5'-TGTTGTCACCAACAAAGTCGG-3' for glyceraldehyde-3-phosphate dehydrogenase (AT1G13440).

Expression and purification of ETHE1

The coding sequence of AT1G53580 was cloned into the pET28a(+) expression vector in frame with a C-terminal 6xHis-tag, using the primers 5'-CATCCATGGGTAAGCTTCTCTTCGTCAACTC-3' and 5'-GCGCCTCGAGGTTGGCTTGAGAAGGCACATC-3'. The first 50 codons containing the mitochondrial targeting sequence were removed and replaced by a Met and Gly codon, generating the N-terminal amino acid sequence MGKLLFRQ. After verification of the nucleotide sequence, the plasmid was transformed into *Escherichia coli* strain BL21(DE3)pLYS. Expression was induced by addition of isopropyl-β-D thiogalactopyranoside to a final concentration of 0.2 mM, followed by incubation at 18°C overnight with shaking. Cell free lysate in 50 mM NaPO₄, 300 mM NaCl, 10 mM imidazole pH 8.0, was applied to a 1 ml His Trap HP column (GE Healthcare) and eluted with a 10 -

250 mM imidazole gradient. ETHE1 purified as a single peak (Supp. Fig. S1A). We obtained a high yield of soluble protein with an electrophoretic mobility of 28 kDa, which is in agreement with the calculated molecular mass of 28,008 Dalton for the monomer (Supp. Fig. S1A). The purified protein contained 0.5 atoms of Fe²⁺ per monomer, as reported previously (McCoy et al., 2006; Tiranti et al., 2009). Pre-incubation of the enzyme with 1 molar equivalent of Fe and addition of 2.5 mM ascorbate did not increase SDO activity. The plasmid containing human ETHE1 was generously provided by Valeria Tiranti and Massimo Zeviani (IRCCS Foundation, Milan) and expressed in the same way as Arabidopsis ETHE1.

Sulfur dioxygenase activity test

SDO activity was measured at 25°C in a Clarke-type oxygen electrode (Oroboros Oxygraph and Hansatech DW1 Oxygraphy) following the procedure described in Hildebrandt and Grieshaber (2008). The reaction contained 1 to 2 µg/ml purified enzyme or 150 to 300 µg/ml mitochondrial protein in 0.1 M KPO₄ pH 7.4. For the standard activity test, 1 mM GSH (final concentration) was added, followed by 15 µl/ml of a saturated elemental sulfur solution in acetone. Acetone did not inhibit enzyme activity. Rates were measured during the linear phase of oxygen depletion, which occurred in the first 2 to 3 minutes.

Phenotype analysis

For general phenotype analysis a modified version of the procedure described in Boyes et al. (2001) was used. Plants were grown under long-day conditions and growth parameters were measured three times per week.

Embryo morphology was analyzed with a microscope equipped with Normarski optics. Siliques were cleared in Hoyer's solution (15 ml distilled water, 3.75 g gum arabic, 2.5 ml glycerine, 50 g chloral hydrate) overnight before seeds were dissected.

Histochemical detection of hydrogen peroxide and superoxide

Histochemical detection of H₂O₂ was performed as described by Thordal-Christensen et al., (1997) with slight modifications: Rosette leaves were incubated in DAB staining solution (1 mg ml⁻¹ 3,3'-diaminobenzidine (DAB), 0.05 % (v/v) Tween 20, 10 mM Na₂HPO₄) for 7 h. Superoxide was detected by formazan staining for 5 h in 0.1 mg mL⁻¹ nitroblue tetrazolium (NBT), 25 mM HEPES, pH 7.6. After DAB or NBT staining, chlorophyll was removed by boiling the leaves in bleaching solution (ethanol:acetic acid:glycerol 3:1:1) for 15 min. H₂O₂

produced a reddish-brown precipitate and superoxide was visualized as a purple formazan deposit within leaf tissues. Stained leaf areas were quantified using ImageJ software (<http://imagej.nih.gov/ij/>).

Metabolite analysis

Products of the SDO reaction were analyzed by HPLC (Hildebrandt and Grieshaber, 2008). Hydrophilic metabolites were extracted from 50 mg leaf material as described by Wirtz and Hell (2003). Derivatization, separation and quantification of thiols, *O*-acetylserine, amino acids and sulfate were performed as described by Heeg et al. (2008). Sulfite, sulfide and thiosulfate were determined according to Birke et al. (2012).

Soluble sugars were extracted from powdered plant material (50 mg) by incubation with 0.5 ml 80% ethanol for 45 min at 80° C. Cell debris and insoluble starch were removed by centrifugation for 10 min at 25.000g and 4°C. Soluble sugars of the resulting supernatant were separated with a gradient of 15 to 300 mM NaOH on a CarboPac PA1 column connected to an ICS-3000 system (Dionex, Germany) and quantified by pulsed amperometric detection (HPAEC-PAD). Data acquisition and quantification was performed with Chromeleon 6.7 (Dionex, Germany). For quantification of starch the sediment of soluble sugar extraction was washed twice with 80% ethanol and resuspended in 0.2 ml 0.2 M KOH. Starch was partly hydrolyzed by incubation at 95°C for 1 h and subsequently digested in 25 mM sodium acetate, pH 5.2 with 0.1 units amyloglucosidase for 16 hours at 37°C. The resulting glucose was quantified by HPAEC-PAD as described above.

Adenylates were quantified as described in Bürstenbinder et al. (2010).

Cell suspension cultures and isolation of mitochondria

Arabidopsis cell suspension cultures were established and maintained as described by May and Leaver (1993) and Sunderhaus et al. (2006). Shortly, *Arabidopsis* seeds were surface sterilized, plated on solid Murashige and Skoog medium (0.44 % (w/v) MS-medium (Duchefa), 2 % (w/v) sucrose, 1 % (w/v) agar, pH 5.7), and grown for 10 days under long-day conditions. Callus formation was induced by incubating stem explants on solid callus induction medium (0.316% (w/v) Gamborg B5 medium (Duchefa), 3% (w/v) sucrose, 1 % (w/v) agar, 0.5 mg l⁻¹ 2,4 dichlorphenoxyacetic acid, 0.05 mg l⁻¹ kinetin, pH 5.7) at 25 °C in the dark. Suspension cultures were grown in 500-ml flasks containing 100 ml of liquid B5 medium (callus induction medium without agar) at 25 °C and 90 rpm in the dark. Cells were transferred into fresh medium every 7 days. There were no significant differences between

growth rates of wild type cells and the *ethe1* mutants. Mitochondria were prepared following to the procedure outlined by Werhahn et al. (2001). The high purity of mitochondria prepared according to this method has been demonstrated by proteome analysis (Kruft et al., 2001).

Mitochondria from cell culture were used to identify the general biochemical function of ETHE1. SDO activity was also measured in mitochondria prepared from rosette leaves of 8-week old wild type Arabidopsis plants grown under short-day conditions following the protocol described in Keech et al. (2005).

Proteomics

One dimensional SDS PAGE and protein blot analysis were carried out following standard methods. Antibodies against purified 6xHis-ETHE1 were produced by Biogenes (Germany), antibodies against O-acetylserine (thiol) lyase, which recognize the three major isoforms of the protein, were used as published (Heeg et al., 2008).

Mitochondrial proteins from wild type and *ethe1-1* cell culture were separated by two-dimensional IEF/SDS PAGE as described in Hildebrandt et al. (2013) with some modifications: 0.5 mg mitochondrial protein from each sample were solubilized by shaking in 450 µl rehydration buffer (6 M urea, 2 M thiourea, 50 mM DTT, 2 % CHAPS (w/v), 5 % IPG buffer 3-11nl (v/v), 12 µl/ml DeStreak reagent, and a trace of bromphenol blue) for 60 min at room temperature. Isoelectric focusing was carried out on Immobiline DryStrip gels (24 cm, non-linear gradient pH 3-11) using the Ettan IPGphor 3 system (GE Healthcare). For the second dimension, the High Performance Electrophoresis FlatTop Tower-System (Serva Electrophoresis) was used with precast tris-glycine gels (12.5 % polyacrylamide, 24 x 20cm). Gel image analysis and protein identification by mass spectrometry were carried out as described in Hildebrandt et al. (2013). Shortly, spots were cut from the 2D gels with a manual spot picker (Genetix), washed in 0.1 M ammonium bicarbonate and dehydrated with acetonitrile. After tryptic digestion peptides were extracted by successive incubation with (i) 50 % v/v acetonitrile, 5 % v/v formic acid (ii-iii) 50 % v/v acetonitrile, 1 % v/v formic acid (iv) 100 % acetonitrile. Nano-HPLC electrospray ionization quadrupole time of flight MS analyses were carried out using an Easy-nLC system (Proxeon) coupled to a microTOF-Q-II mass spectrometer (Bruker Daltonics). LC separation was achieved with a C18 reverse phase column (Proxeon EASY-Column, length = 10 cm, i.d. = 75 µm; ReproSil-Pur C18-AQ, 3 µm, 120 Å) coupled to a Proxeon EASY-PreColumn (length = 2 cm, i.d. = 100 µm; ReproSil-Pur C18-AQ, 5 µm, 120 Å) using an acetonitrile/formic acid gradient (Klodmann et al., 2011).

MS/MS fragmentation was carried out automatically. Proteins were identified using the MASCOT search algorithm against Tair 10 (www.arabidopsis.org).

Miscellaneous methods

A co-expression analysis based on a manually curated database of 40k microarrays was performed with Genevestigator (www.genevestigator.com; Nebion, Hurz et al., 2008). Genes that are co-regulated with *ATIG53580* under relevant conditions were identified following a two-step workflow. First, experiments with a significant change ($p < 0.05$) of at least 1.5-fold in *ETHE1* expression were selected using the perturbations tool. The 100 genes with most similar expression patterns in these experiments were then identified with the co-expression tool using the Pearson correlation coefficient as the measure of similarity.

Protein was quantified using the BioRad Protein Assay reagent, iron was quantified using the colorimetric chelator ferene (Hennessy et al., 1984).

Supplemental material

Supplemental Figure S1. Purification, pH and temperature optima of Arabidopsis and human ETHE1.

Supplemental Figure S2. Growth parameters of *ethe1-1* and wild type rosettes under long-day conditions.

Supplemental Figure S3. Identification of proteins with altered abundance in mitochondria of *ethe1-1* compared to wild type.

Supplemental Figure S4. Leaf senescence in wild type and *ethe1-1* plants under long-day and short-day growth conditions.

Supplemental Figure S5. Histochemical detection of reactive oxygen and sulfur species in leaves of wild type and *ethe1-1* plants.

Supplemental Table S1. Identification of substrates for recombinant ETHE1 and the SDO reaction in Arabidopsis mitochondria.

Supplemental Table S2. Identification of proteins with altered abundance in mitochondria of *ethe1-1* compared to wild type.

Supplemental Table S3. Genes that are co-expressed with ETHE1 in Arabidopsis under relevant conditions.

Supplemental Table S4. Amino acid and GSH contents of wild type and *ethe1-1* seeds at 4-5 DAP.

Supplemental Table S5. Metabolite contents of wild type and *ethe1-1* rosette leaves under long-day and short-day growth conditions as well as after extended darkness.

Supplemental Table S6. Contents of sulfite, thiosulfate, and sulfide in wild type and *ethe1* mutant rosette leaves after 7 days of extended darkness.

ACKNOWLEDGEMENTS

We thank Valeria Tiranti and Massimo Zeviani for providing the plasmid for expression of human ETHE1, Christoph Peterhänsel and Steffanie Fromm for assistance with PCR experiments, Herbert Geyer and Jens-Peter Barth for taking care of the plants, Traud Winkelmann for support with the microscope, Mascha Brinkötter for taking part in histochemical ROS detection, and Lorna Jackson for optimizing the immunodetection of ETHE1 protein. We thank the Metabolomics Core Technology Platform of the Excellence cluster “CellNetworks” (University of Heidelberg) and the Deutsche Forschungsgemeinschaft (grant ZUK 40/2010-3009262) for support with HPLC-based metabolite quantification.

LITERATURE CITED

- Alvarez C, Calo L, Romero LC, Garcia I, Gotor C** (2010) An O-acetylserine(thiol)lyase homolog with L-cysteine desulfhydrase activity regulates cysteine homeostasis in Arabidopsis. *Plant Physiol* **152**: 656–669
- Alvarez C, Garcia I, Moreno I, Perez-Perez ME, Crespo JL, Romero LC, Gotor C** (2012) Cysteine-generated sulfide in the cytosol negatively regulates autophagy and modulates the transcriptional profile in Arabidopsis. *Plant Cell* **24**: 4621–4634
- Araújo WL, Ishizaki K, Nunes-Nesi A, Larson TR, Tohge T, Krahnert I, Witt S, Obata T, Schauer N, Graham IA, Leaver CJ, Fernie AR** (2010) Identification of the 2-hydroxyglutarate and isovaleryl-CoA dehydrogenases as alternative electron donors linking lysine catabolism to the electron transport chain of Arabidopsis mitochondria. *Plant Cell* **22**: 1549–1563
- Araújo WL, Tohge T, Ishizaki K, Leaver CJ, Fernie AR** (2011) Protein degradation – an alternative respiratory substrate for stressed plants. *Trends Plant Sci* **16**: 489–498
- Baena-González E, Rolland F, Thevelein JM, Sheen J** (2007) A central integrator of transcription networks in plant stress and energy signalling. *Nature* **448**: 938–942
- Balk J, Pilon M** (2011) Ancient and essential: the assembly of iron–sulfur clusters in plants. *Trends Plant Sci* **16**: 218–226
- Birke H, Haas F, Kok L de, Balk J, Wirtz M, Hell R** (2012) Cysteine biosynthesis, in concert with a novel mechanism, contributes to sulfide detoxification in mitochondria of Arabidopsis thaliana. *Biochem J* **445**: 275–283
- Boyes DC, Zayed AM, Ascenzi R, McCaskill AJ, Hoffman NE, Davis KR** (2001) Growth stage–based phenotypic analysis of Arabidopsis: A model for high throughput functional genomics in plants. *Plant Cell* **13**: 1499–1510
- Brychkova G, Grishkevich V, Fluhr R, Sagi M** (2012) An essential role for tomato sulfite oxidase and enzymes of the sulfite network in maintaining leaf sulfite homeostasis. *Plant Physiol* **161**: 148–164
- Buchner P, Stuiver CEE, Westerman S, Wirtz M, Hell R, Hawkesford MJ, de Kok LJ** (2004) Regulation of sulfate uptake and expression of sulfate transporter genes in *Brassica oleracea* as affected by atmospheric H₂S and pedospheric sulfate nutrition. *Plant Physiol* **136**: 3396–3408
- Bürstenbinder K, Waduwara I, Schoor S, Moffatt BA, Wirtz M, Minocha SC, Oppermann Y, Bouchereau A, Hell R, Sauter M** (2010) Inhibition of 5'-methylthioadenosine metabolism in the Yang cycle alters polyamine levels, and impairs seedling growth and reproduction in Arabidopsis. *Plant J* **62**: 977–988
- Di Meo I, Fagiolarì G, Prella A, Viscomi C, Zeviani M, Tiranti V** (2011) Chronic exposure to sulfide causes accelerated degradation of cytochrome c oxidase in ethylmalonic encephalopathy. *Antioxid Redox Signal* **15**: 353–362
- Dooley FD, Nair SP, Ward PD, Rutherford S** (2013) Increased growth and germination success in plants following hydrogen sulfide administration. *PLoS ONE* **8**: e62048
- Fahnenstich H, Saigo M, Niessen M, Zanon MI, Andreo CS, Fernie AR, Drincovich MF, Flugge U, Maurino VG** (2007) Alteration of organic acid metabolism in Arabidopsis overexpressing the maize C4 NADP-malic enzyme causes accelerated senescence during extended darkness. *Plant Physiol* **145**: 640–652
- García-Mata C, Lamattina L** (2010) Hydrogen sulphide, a novel gasotransmitter involved in guard cell signalling. *New Phytologist* **188**: 977–984

- Geisler DA, Papke C, Obata T, Nunes-Nesi A, Matthes A, Schneitz K, Maximova E, Araujo WL, Fernie AR, Persson S** (2012) Downregulation of the δ -subunit reduces mitochondrial ATP synthase levels, alters respiration, and restricts growth and gametophyte development in *Arabidopsis*. *Plant Cell* **24**: 2792–2811
- Giordano C, Viscomi C, Orlandi M, Papoff P, Spalice A, Burlina A, Meo I, Tiranti V, Leuzzi V, d'Amati G, Zeviani M** (2012) Morphologic evidence of diffuse vascular damage in human and in the experimental model of ethylmalonic encephalopathy. *J Inher Metab Dis* **35**: 451–458
- Gu L, Jones AD, Last RL** (2010) Broad connections in the *Arabidopsis* seed metabolic network revealed by metabolite profiling of an amino acid catabolism mutant. *Plant J* **61**: 579–590
- Hatzfeld Y, Maruyama A, Schmidt A, Noji M, Ishizawa K, Saito K** (2000) Beta-cyanoalanine synthase is a mitochondrial cysteine synthase-like protein in spinach and *Arabidopsis*. *Plant Physiol* **123**: 1163–1172
- Heeg C, Kruse C, Jost R, Gutensohn M, Ruppert T, Wirtz M, Hell R** (2008) Analysis of the *Arabidopsis* O-acetylserine(thiol)lyase gene family demonstrates compartment-specific differences in the regulation of cysteine synthesis. *Plant Cell* **20**: 168–185
- Hell R, Wirtz M** (2011) Molecular biology, biochemistry and cellular physiology of cysteine metabolism in *Arabidopsis thaliana*. *The Arabidopsis Book* **9**: e0154
- Hennessy DJ, Reid GR, Smith FE, Thompson SL** (1984) Ferene - a new spectrophotometric reagent for iron. *Can J Chem* **62**: 721–724
- Hildebrandt TM, Di Meo I, Zeviani M, Viscomi C, Braun H-P** (2013) Proteome adaptations in Eth1-deficient mice indicate a role in lipid catabolism and cytoskeleton organization via post-translational protein modifications. *Biosci Rep* **33**: 575–584
- Hildebrandt TM, Grieshaber MK** (2008) Three enzymatic activities catalyze the oxidation of sulfide to thiosulfate in mammalian and invertebrate mitochondria. *FEBS J* **275**: 3352–3361
- Holdorf MM, Owen HA, Lieber SR, Yuan L, Adams N, Dabney-Smith C, Makaroff CA** (2012) *Arabidopsis* ETHE1 encodes a sulfur dioxygenase that is essential for embryo and endosperm development. *Plant Physiol* **160**: 226–236
- Hruz T, Laule O, Szabo G, Wessendorp F, Bleuler S, Oertle L, Widmayer P, Gruissem W, Zimmermann P** (2008) Genevestigator V3: A reference expression database for the meta-analysis of transcriptomes. *Advances in Bioinformatics* **2008**: 1–5
- Ishizaki K, Larson TR, Schauer N, Fernie AR, Graham IA, Leaver CJ** (2005) The critical role of *Arabidopsis* electron-transfer flavoprotein:ubiquinone oxidoreductase during dark-induced starvation. *Plant Cell* **17**: 2587–2600
- Ishizaki K, Schauer N, Larson TR, Graham IA, Fernie AR, Leaver CJ** (2006) The mitochondrial electron transfer flavoprotein complex is essential for survival of *Arabidopsis* in extended darkness. *Plant J* **47**: 751–760
- Izumi M, Hidema J, Makino A, Ishida H** (2013) Autophagy contributes to nighttime energy availability for growth in *Arabidopsis*. *Plant Physiol* **161**: 1682–1693
- Jander G, Norris SR, Joshi V, Fraga M, Rugg A, Yu S, Li L, Last RL** (2004) Application of a high-throughput HPLC-MS/MS assay to *Arabidopsis* mutant screening; evidence that threonine aldolase plays a role in seed nutritional quality. *Plant J* **39**: 465–475
- Jin Z, Shen J, Qiao Z, Yang G, Wang R, Pei Y** (2011) Hydrogen sulfide improves drought resistance in *Arabidopsis thaliana*. *Biochem Biophys Res Com* **414**: 481–486

- Jin Z, Xue S, Luo Y, Tian B, Fang H, Li H, Pei Y** (2013) Hydrogen sulfide interacting with abscisic acid in stomatal regulation responses to drought stress in *Arabidopsis*. *Plant Physiol Biochem* **62**: 41–46
- Kabil O, Banerjee R** (2012) Characterization of patient mutations in human persulfide dioxygenase (ETHE1) involved in H₂S catabolism. *J Biol Chem* **287**: 44561–44567
- Keech O, Dizengremel P, Gardeström P** (2005) Preparation of leaf mitochondria from *Arabidopsis thaliana*. *Physiologia Plantarum* **124**: 403–409
- Klodmann J, Senkler M, Rode C, Braun HP** (2011) Defining the protein complex proteome of plant mitochondria. *Plant Physiol* **157**: 587–598
- Kruft V, Eubel H, Jansch L, Werhahn W, Braun HP** (2001) Proteomic approach to identify novel mitochondrial proteins in *Arabidopsis*. *Plant Physiol* **127**: 1694–1710
- Lang C, Popko J, Wirtz M, Hell R, Herschbach C, Kreuzwieser J, Rennenberg H, Mendel RR, Hänsch R** (2007) Sulphite oxidase as key enzyme for protecting plants against sulphur dioxide. *Plant Cell Environ* **30**: 447–455
- Li F, Vierstra RD** (2012) Autophagy: a multifaceted intracellular system for bulk and selective recycling. *Trends Plant Sci* **17**: 526–537
- Li Z, Gong M, Xie H, Yang L, Li J** (2012) Hydrogen sulfide donor sodium hydrosulfide-induced heat tolerance in tobacco (*Nicotiana tabacum* L) suspension cultured cells and involvement of Ca²⁺ and calmodulin. *Plant Sci* **185-186**: 185–189
- Mao G, Wang R, Guan Y, Liu Y, Zhang S** (2011) Sulfurtransferases 1 and 2 play essential roles in embryo and seed development in *Arabidopsis thaliana*. *J Biol Chem* **286**: 7548–7557
- May MJ, Leaver CJ** (1993) Oxidative stimulation of glutathione synthesis in *Arabidopsis thaliana* suspension cultures. *Plant Physiol* **103**: 621–627
- McCoy JG, Bingman CA, Bitto E, Holdorf MM, Makaroff CA, Phillips GN** (2006) Structure of an ETHE1-like protein from *Arabidopsis thaliana*. *Acta Crystallogr D Biol Crystallogr* **62**: 964–970
- Niessen M, Krause K, Horst I, Staebler N, Klaus S, Gaertner S, Kebeish R, Araujo WL, Fernie AR, Peterhänsel C** (2012) Two alanine aminotransferases link mitochondrial glycolate oxidation to the major photorespiratory pathway in *Arabidopsis* and rice. *J Exp Bot* **63**: 2705–2716
- Riemenschneider A, Wegele R, Schmidt A, Papenbrock J** (2005) Isolation and characterization of a D-cysteine desulfhydrase protein from *Arabidopsis thaliana*. *FEBS J* **272**: 1291–1304
- Robison MM, Ling X, Smid MPL, Zarei A, Wolyn DJ** (2009) Antisense expression of mitochondrial ATP synthase subunits OSCP (ATP5) and γ (ATP3) alters leaf morphology, metabolism and gene expression in *Arabidopsis*. *Plant Cell Physiol* **50**: 1840–1850
- Rohwerder T, Sand W** (2003) The sulfane sulfur of persulfides is the actual substrate of the sulfur-oxidizing enzymes from *Acidithiobacillus* and *Acidiphilium spp.* *Microbiology* **149**: 1699–1710
- Shaw L, Engel PC** (1987) CoA-persulphide: a possible in vivo inhibitor of mammalian short-chain acyl-CoA dehydrogenase. *Biochim Biophys Acta* **919**: 171–174
- Sunderhaus S, Dudkina NV, Jansch L, Klodmann J, Heinemeyer J, Perales M, Zabaleta E, Boekema EJ, Braun H-P** (2006) Carbonic anhydrase subunits form a matrix-exposed domain attached to the membrane arm of mitochondrial complex I in plants. *J Biol Chem* **281**: 6482–6488
- Szal B, Dąbrowska Z, Malmberg G, Gardeström P, Rychter AM** (2008) Changes in energy status of leaf cells as a consequence of mitochondrial genome rearrangement. *Planta* **227**: 697–706

- Taylor NL, Heazlewood JL, Day DA, Millar AH** (2004) Lipoic acid-dependent oxidative catabolism of α -keto acids in mitochondria provides evidence for branched-chain amino acid catabolism in Arabidopsis. *Plant Physiol* **134**: 838–848
- Thordal-Christensen H, Zhang Z, Wei Y, Collinge DB** (1997) Subcellular localization of H₂O₂ in plants. H₂O₂ accumulation in papillae and hypersensitive response during the barley - powdery mildew interaction. *Plant J* **11**: 1187–1194
- Tiranti V, D'Adamo P, Briem E, Ferrari G, Mineri R, Lamantea E, Mandel H, Balestri P, Garcia-Silva M, Vollmer B, Rinaldo P, Hahn SH, Leonard J, Rahmam S, Dionisi-Vici C, Garavaglia B, Gasparini P, Zeviani M** (2004) Ethylmalonic encephalopathy is caused by mutations in ETHE1, a gene encoding a mitochondrial matrix protein. *Am J Hum Genet* **74**: 239–252
- Tiranti V, Viscomi C, Hildebrandt T, Di Meo I, Mineri R, Tiveron C, D Levitt M, Prella A, Fagiolari G, Rimoldi M, Zeviani M** (2009) Loss of ETHE1, a mitochondrial dioxygenase, causes fatal sulfide toxicity in ethylmalonic encephalopathy. *Nat Med* **15**: 200–205
- van Hoewyk D, Pilon M, Pilon-Smits EA** (2008) The functions of NifS-like proteins in plant sulfur and selenium metabolism. *Plant Sci* **174**: 117–123
- Werhahn W, Niemeyer A, Jansch L, Kruft V, Schmitz U, Braun H-P** (2001) Purification and characterization of the preprotein translocase of the outer mitochondrial membrane from Arabidopsis. Identification of multiple forms of TOM20. *Plant Physiol* **125**: 943–954
- Wirtz M, Hell R** (2003) Production of cysteine for bacterial and plant biotechnology: application of cysteine feedback-insensitive isoforms of serine acetyltransferase. *Amino Acids* **24**: 195–203
- Zhang H, Hu L, Hu K, He Y, Wang S, Luo J** (2008) Hydrogen sulfide promotes wheat seed germination and alleviates oxidative damage against copper stress. *J Integr Plant Biol* **50**: 1518–1529
- Zhang H, Tan Z, Hu L, Wang S, Luo J, Jones RL** (2010) Hydrogen sulfide alleviates aluminum toxicity in germinating wheat seedlings. *J Integr Plant Biol* **52**: 556–567
- Zhu X, Tang G, Granier F, Bouchez D, Galili G** (2001) A T-DNA insertion knockout of the bifunctional lysine- α -ketoglutarate reductase/saccharopine dehydrogenase gene elevates lysine levels in Arabidopsis seeds. *Plant Physiol* **126**: 1539–1545

Figure legends

Figure 1. Molecular characterization of the T-DNA insertion lines *ethe1-1*, *ethe1-2* and *ethe1-3*

(A) Genomic structure of the *ETHE1* gene and positions of T-DNA insertions in the mutant lines (white triangles). (B) *ETHE1* expression in *ethe1* mutants was quantified relative to wild type (wt) by RT-qPCR (n = 5). Cytosolic *GAPDH* (AT1G13440) was used for normalization. (C) Immunological detection of ETHE1 protein in mitochondria isolated from cell suspension cultures of wild type and the *ethe1* mutants. Purity of the mitochondrial fraction was confirmed using an O-acetylserine (thiol) lyase (OAS-TL) antibody. This antibody recognizes OAS-TL isoforms localized in the mitochondria, the plastids and the cytosol, the latter of which are slightly smaller than the mitochondrial isoform. Absence of the additional bands is taken for evidence of the purity of the mitochondrial fraction. Ponceau S-stained protein was used as loading control. (D) Sulfur dioxygenase activity was determined in the mitochondria described in (C) (n = 5-10). Mean values \pm SD are shown. * Significantly different ($P < 0.05$) from the wild type, Student's t-test.

Figure 2. Substrates and products of ETHE1

(A) SDO activity of recombinant ETHE1 was measured as oxygen consumption using a Clarke-type oxygen electrode. 1 mM reduced glutathione (GSH) plus 15 μ l/ml saturated acetic solution of elemental sulfur (S₈), 3 mM Na₂S plus 0.5 mM oxidized glutathione (GSSG) preincubated at 30°C for 10 min, and 5 mM 3-mercaptopyruvate (3MP) plus 1 mM GSH were used as substrates (n = 3). (B) Original traces of an SDO activity test for recombinant ETHE1 (1.5 μ g protein/ml). 1 mM GSH and 15 μ l/ml saturated acetic solution of elemental sulfur (S₈) were added (indicated by arrows) to produce the substrate GSSH non-enzymatically. The oxygen concentration was measured using an oxygen electrode and concentrations of sulfite and thiosulfate were quantified by HPLC. (C) SDO activity of mitochondria isolated from wild type, *ethe1-1* and *ethe1-3* cell suspension cultures was measured as oxygen consumption. 1 mM GSH plus 15 μ l/ml S₈, 1 mM NaHS plus 1 mM GSSG, and 5 mM 3MP were used as substrates (n = 3). (D) Original traces of an SDO activity test for wild type Arabidopsis mitochondria (0.25 mg protein/ml). Conditions were the same as in (B). * Significantly different ($P < 0.05$) from the wild type, Student's t-test.

Figure 3. Products of sulfide metabolism in wild type and *ethe1-1* plants

Sulfur containing metabolites were extracted from aerial parts of wild type and *ethe1-1* plants grown under short-day conditions for 4 weeks followed by exposure to 0 (-) or 1 (+) ppm H₂S for 12 days and quantified using HPLC (n = 3). FW, fresh weight; OAS, O-acetylserine; GSH, reduced glutathione. * Significantly different (P < 0.05) from the wild type, Student's t-test.

Figure 4. Phenotype of *ETHE1* knockdown mutants grown under long-day conditions

(A) Representative pictures of embryos in seeds of wild type plants and *ethe1-1* mutants at 5 and 7 days after pollination (DAP). Scale bar = 50 μm. (B) Progression of embryo development in wild type and *ethe1-1*. A total of 224 siliques between 1 and 12 DAP from 4 different plants were analyzed for wt and mutant respectively and bars indicate the mean age ± standard deviation of embryos in the different developmental stages. (C) Rosettes of wild type plants and the *ethe1* mutant lines 40 days after sowing. (D) Mature wild type and mutant plants 56 days after sowing. (E) Principle growth stages according to Boyes et al. (2001). Bars represent mean values for the duration of the stages for wild type plants and *ethe1* mutant lines (n = 10). * Significantly different (P < 0.05) from the wild type, Mann-Whitney Rank Sum Test.

Figure 5. Phenotype and metabolite profile of wild type and *ethe1-1* plants under condition stimulating protein degradation

Rosettes of wild type and *ethe1-1* plants (A) after 13 weeks of growth under long-day conditions (ld: 16 h light/8 h dark), (B) after 7 weeks of growth under short-day conditions (sd: 8 h light/16 h dark) and (C) after 7 days of extended darkness (ed) following 7 weeks of growth under short-day conditions. (D) Amino acids and GSH, carbohydrates, and adenylates were extracted from rosette leaves of wild type and *ethe1-1* plants grown under the conditions shown in A-C and quantified using HPLC (n = 5). Σ = sum of all detectable free amino acids, starch content is shown as glucose equivalents. * Significantly different (P < 0.05) from the wild type, Student's t-test. For complete amino acid, carbohydrate and adenylate profiles see Supp. Tab. S5 (E) Relative *ETHE1* transcript levels in rosette leaves of wild type plants during the conditions shown in A-C were determined by RT-qPCR (n = 5). Transcript levels of *ETHE1* were normalized to cytosolic *GAPDH* (AT1G13440).

Figure 6. Model of cysteine catabolic pathways in *Arabidopsis thaliana*

In the cytosol cysteine is desulfurated by L-cysteine desulfhydrase (DES1) producing hydrogen sulfide (H₂S). Sulfide is oxidized to glutathione persulfide (GSSH) either non-enzymatically in the presence of oxidized glutathione (GSSG) or catalyzed by a currently unknown cytosolic enzyme. In the mitochondrial matrix cysteine is converted to 3-mercaptopyruvate (3-MP) by an aminotransferase (AAT) before a sulfurtransferase (STR1) transfers the persulfide group to an acceptor such as GSH producing GSSH. ETHE1 oxidizes GSSH to sulfite (SO₃²⁻), which is either converted to thiosulfate (S₂O₃²⁻) via addition of a persulfide group by a mitochondrial sulfurtransferase (STR1) or transported to the peroxisomes for oxidation to sulfate (SO₄²⁻) by sulfite oxidase (SO) (Lang et al., 2007; Brychkova et al., 2012).

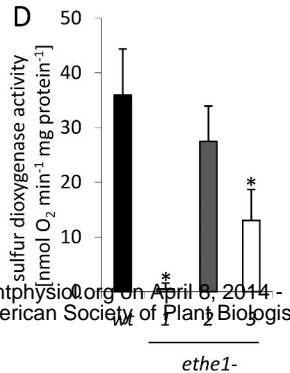
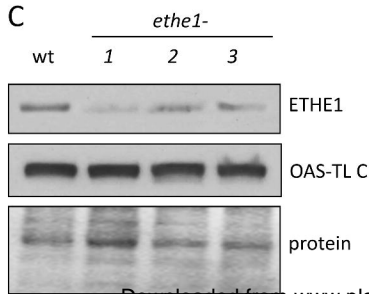
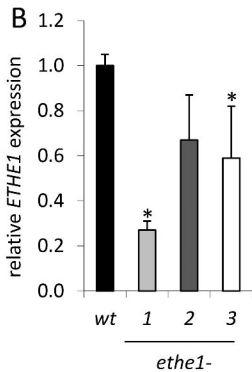
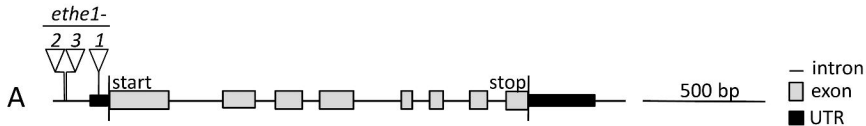
Tables

Table 1. Proteins with potentially changed abundance in *ethe1-1* mitochondria

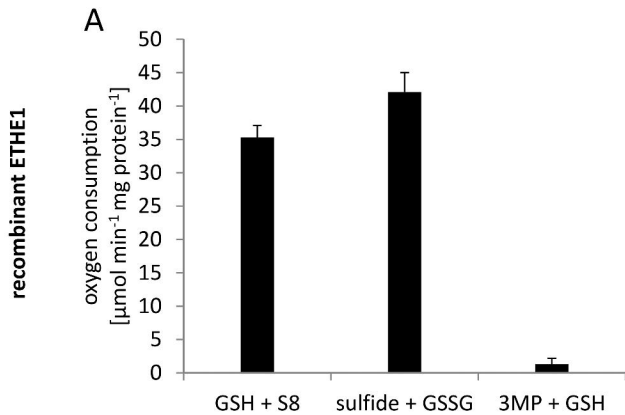
Mitochondrial proteins from wild type and *ethe1-1* cell culture were separated by IEF/SDS PAGE (Supp. Fig. S3). Gels from 3 biological replicates were analyzed by Delta2D and the proteins in spots with at least 1.5-fold changes in volume were identified by nanoLC-MS/MS. For additional information see Supplemental Table S2

Spot	Accession	Name	Ratio ^a	Spot	Accession	Name	Ratio ^a
1	AT3G55410	E1 2-oxoglutarate DH	4.23	25	AT1G51390	NifU5	0.66
2	AT3G61440	beta-cyanoalanine synthase	3.98	26	AT5G07440	Glutamate DH	0.63
3	AT2G05710	Aconitase	3.06	27	AT1G65290	Acyl carrier protein	0.63
4	AT3G10920	Superoxide dismutase [Mn]	2.92	28	AT1G06530	Tropomyosin-related protein	0.63
5	AT3G55410	E1 2-oxoglutarate DH	2.90	28	AT4G26780	Chaperone GrpE	0.63
6	AT2G29530	Tim10	2.54	29	AT2G30970	Aspartate aminotransferase	0.62
7	AT2G45060	hypothetical protein	2.41	30	AT3G20970	NifU 4	0.61
7	AT1G53240	Malate dehydrogenase	2.41	31	AT2G28000	Chaperonin 60 alpha	0.61
7	AT2G30920	Hexaprenyl... methyltransferase	2.41	31	AT3G02650	TPR-like protein	0.61
7	AT3G18580	Single-strand DNA-binding protein	2.41	32	AT4G35090	Catalase	0.61
7	AT5G13450	ATP synthase subunit O	2.41	33	AT5G62690	Tubulin	0.60
7	AT4G26910	E2 2-oxoglutarate DH	2.41	34	AT5G66760	Succinate DH	0.60
7	AT5G23140	Clp protease	2.41	35	AT2G07698	ATP synthase subunit alpha	0.58
8	AT5G18170	Glutamate dehydrogenase	2.41	35	AT1G48030	E3 dihydrolipoyl DH	0.58
9	AT5G26780	Serine hydroxymethyltransferase	2.38	36	AT2G43400	ETFQO	0.58
9	AT5G62530	Deltapyrroline-5-carboxylate DH	2.38	37	AT3G58610	Ketol-acid reductoisomerase	0.55
10	AT2G42210	Tim17 domain-containing protein	2.36	38	AT2G33210	Chaperonin CPN60	0.53
11	AT4G34030	Methylcrotonyl-CoA carboxylase	2.17	38	AT5G04740	ACT domain-containing protein	0.53
12	AT3G06850	E2 BCKDH	2.04	39	AT2G43090	3-Isopropylmalate dehydratase	0.50
13	AT3G13930	E2 Pyruvate dehydrogenase	2.01	40	AT3G23990	Chaperonin CPN60	0.49
14	AT5G65750	E1 2-oxoglutarate dehydrogenase	1.96	41	AT3G43810	Calmodulin	0.37
14	AT2G22780	Malate dehydrogenase	1.96	42	AT1G22300	GRF10 (14-3-3-like)	0.37
15	AT3G02780	Isopentenyl-diph. delta-isomerase	1.89	42	AT5G38480	GRF3 (14-3-3-like)	0.37
15	AT2G21870	ATP synthase subunit	1.89	42	AT4G22240	Lipid-associated protein	0.37
16	AT4G05400	Copper ion binding protein	1.84	43	AT1G54580	Acyl carrier protein	0.29
17	AT4G34700	Complex I beta subcomplex 9	1.83	44	AT4G24280	HSP70-1	0.28
18	AT5G08530	Complex I flavoprotein 1	1.73	45	AT1G66410	Calmodulin	0.24
18	AT2G07698	ATP synthase subunit alpha	1.73				
19	AT3G13110	Serine acetyltransferase (SAT)	1.66				
19	AT3G26760	Rossmann-fold containing protein	1.66				
19	AT5G20080	NADH-cytochrome b5 reductase	1.66				
19	AT5G63400	Adenylate kinase	1.66				
20	AT5G66510	Gamma carbonic anhydrase	1.64				
20	AT5G43430	Electron transfer flavoprotein	1.64				
20	AT5G15090	VDAC3	1.64				
21	AT2G05710	Aconitase	1.62				
21	AT5G08670	ATP synthase subunit beta	1.62				
21	AT3G17240	E3 Dihydrolipoyl DH	1.62				
21	AT1G63940	Monodehydroascorbate reductase	1.62				
22	AT3G18580	Single-strand DNA binding protein	1.62				
22	AT2G31140	Peptidase	1.62				
22	AT4G15640	Unknown protein	1.62				
22	AT4G15940	Fumarylacetoacetate hydrolase	1.62				
22	AT5G13450	ATP synthase subunit O	1.62				
23	AT5G65720	Cysteine desulfurase (NifS)	1.60				
24	AT5G26780	Serine hydroxymethyltransferase	1.53				

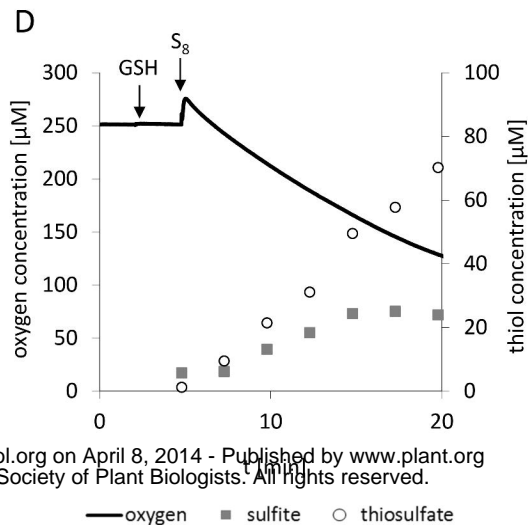
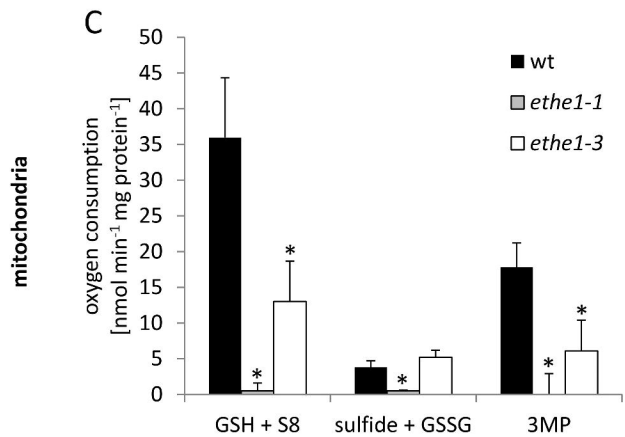
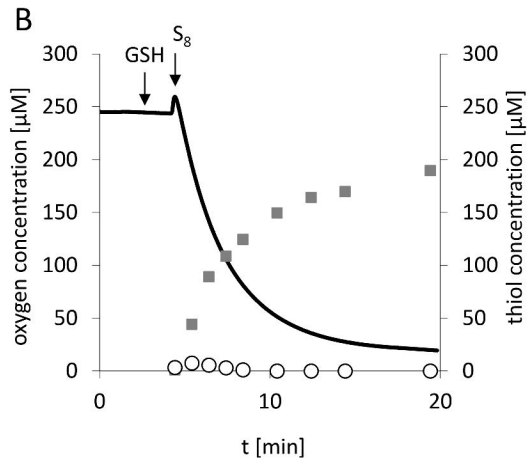
^a Ratio of mean spot volume in *ethe1-1* gels/mean spot volume in wild type gels

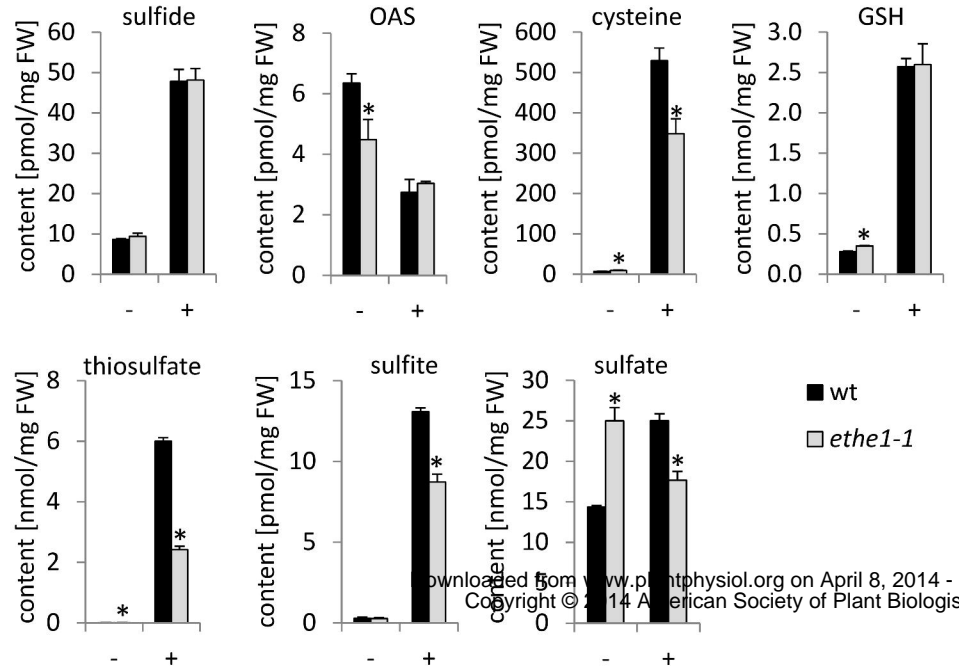


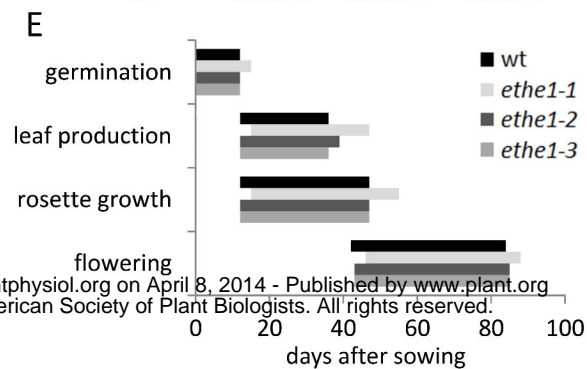
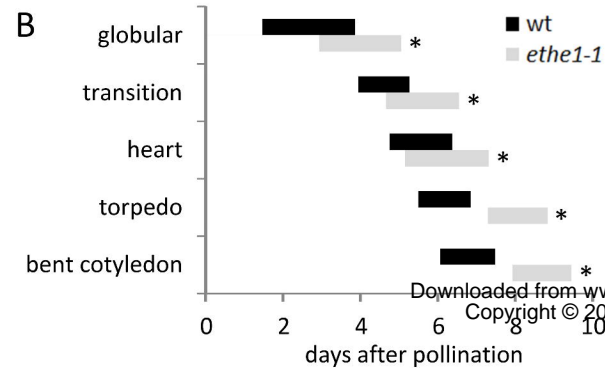
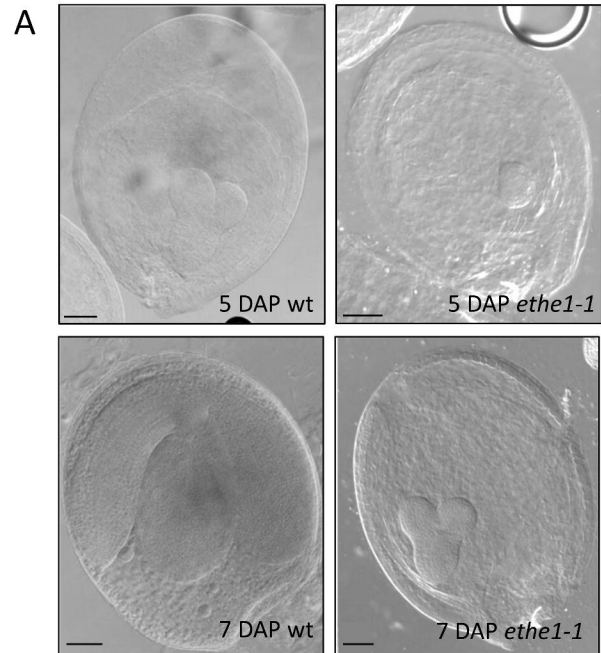
substrates



products







A long-day (ld)



B short-day (sd)



C extended darkness (ed)



D

